Bulk regeneration of optical fiber Bragg gratings

Li-Yang Shao,[1,2] Tao Wang,[1,3] John Canning,[1,*] Kevin Cook,[1] and Hwa-Yaw Tam[2]

[1]Interdisciplinary Photonics Laboratories (iPL), School of Chemistry, University of Sydney, New South Wales 2006, Australia

[2]Department of Electrical Engineering, The Hong Kong Polytechnic University, Hung Hom, Kowloon, Hong Kong SAR, China

[3]Institute of Optoelectronic Technology, Beijing Jiaotong University, Beijing 100044, China

*Corresponding author: john.canning@sydney.edu.au

Received 10 August 2012; accepted 9 September 2012;
posted 18 September 2012 (Doc. ID 174143); published 11 October 2012

The reliability and reproducibility of regenerated gratings for mass production is assessed through simultaneous bulk regeneration of 10 gratings. The gratings are characterized and variations are compared after each stage of fabrication, including seed (room-temperature UV fabrication), regeneration (annealing at 850°C), and postannealing (annealing at 1100°C). In terms of Bragg wavelength (λ_B), the seed grating variation lies within $\Delta\lambda_B = 0.16$ nm, the regenerated grating within $\Delta\lambda_B = 0.41$ nm, and the postannealed grating within $\Delta\lambda_B = 1.42$ nm. All the results are within reasonable error, indicating that mass production is feasible. The observable spread in parameters from seed to regenerated grating is clearly systematic. The postannealed spread arises from the small tension on the fiber during postannealing and can be explained by the softening of the glass when the strain temperature of silica is reached.

OCIS codes: 060.3735, 060.3738, 060.2370, 120.6780, 130.6010.

1. Introduction

High-temperature optical fiber sensors are desirable for many harsh environmental applications, including, for example, the oil and gas industries [1], the monitoring of engine turbines and furnaces [2], and as thermally stable feedback elements and temperature monitors within high-power lasers for material processing [3]. Conventional fiber Bragg gratings are optimized to operate up to 80°C for 25 years, which meets the needs of the telecommunications industry. In sensing applications, a variety of techniques have been employed to raise this temperature performance, whether through varying the optical fiber composition [4], thermal stabilization by preannealing [5] and stress relaxation [6], hypersensitization through an initial optimized irradiation [7], continued exposure into a negative index regime [8], localized and low loss damage ideally through multiphoton femtosecond laser fabrication [9], and regeneration [10,11].

Regeneration is a dramatic process taking conventional type I gratings as "seeds," annealing them out at high temperature and forming reborn, stable gratings. It can be divided into two cases, with and without hydrogen loading in the seed grating. For the case of no hydrogen, the dominant grating structure change is related to the dopant content of the core, and thermal type 1n (type IIA) grating formation is obtained [12]. This increases the stability to similar levels as laser induced "negative" type 1n gratings—up to 700°C or so [8]. In the presence of hydrogen, regeneration occurs at higher temperatures, and the thermal stability is tremendously improved, consistent with changes in silica rather than the dopants. The mechanism is therefore distinct and rests with tensile stress relaxation in the presence of hydrogen by physical inhibition of relaxation causing internal strains opposing the initial core–cladding tensile stress. The condition of regeneration appears to strongly correlate with differences in glass relaxation between the cladding and core, which is softened

1559-128X/12/307165-05$15.00/0

above 800°C. Postannealing of regenerated grating to above the strain temperature of silica helps to stabilize the changes further [11,13]. However, given the apparent complexity of the processes, no systematic work has been done to study the possibility of mass production of regenerated gratings for practical high-temperature industrial applications.

In this work, we aim to investigate the feasibility of mass production of regenerated gratings where individual interrogation and characterization is only carried out post fabrication. This helps to determine the reproducibility and accuracy of the production method. Simultaneous bulk regeneration of 10 gratings are characterized at each stage of fabrication, and variations are compared among seed gratings that are fabricated by UV exposure at room temperature 25°C, regenerated-only ones (fabricated by annealing at 850°C), and postannealed ones (annealing at 1100°C). We demonstrate that the additional thermal processing time is only a moderate extension of normal grating writing given that a bulk quantity of gratings can be regenerated simultaneously. The variation of postannealed gratings is much larger than that of regenerated-only ones, which arises from the small tension on the fiber during postannealing and can be explained by the relaxation of the glass once the strain temperature of silica is reached.

2. Experiments

A. Seed Grating Fabrication

Hydrogen loading in optical fibers not only improves their photosensitivity through hydride and hydroxyl formation, essential for writing strong seed gratings and therefore stronger regenerated gratings, it also plays a mechanical role in reducing tensile stress through dilation, which enables and accelerates the regeneration process [14]. A direct correlation between seed grating strength and regenerated grating strengths has been demonstrated [15]. Boron-codoped germanosilicate fiber (GF1) ($[GeO_2] \sim 30$ mol. %, $[B_2O_3] \sim 12$ mol.%) was used to fabricate strong seed gratings, which was H_2-loaded prior to grating writing ($P = 180$ atm, $T = 80°C$, $t = 2$ days). Uniform Bragg gratings were inscribed into the GF1 fiber by direct writing through an optical phase mask over 1 cm with 193 nm from an ArF laser ($E_{\text{pulse}} = 95$ mJ/cm^2, $f_{\text{cum}} = 7.0$ J/cm^2, RR = 30 Hz, $\tau_w = 15$ ns). Figure 1 shows the refractive index changes as a function of exposure dose of hydrogen-loaded GF1 fiber irradiated using 193 nm pulsed ArF laser. Because of the high germanium doping in the fiber core, the reflection strength, R, of the grating grows rapidly. The average refractive index change Δn_{av} can be calculated from the Bragg wavelength λ_B of the grating, the shift of the measured Bragg wavelength $\Delta\lambda_B$, the effective refractive index n_{eff}, and the overlap factor η [16]:

$$\Delta n_{\text{av}} = \frac{\Delta\lambda_B \cdot n_{\text{eff}}}{\eta \cdot \lambda_B}. \quad (1)$$

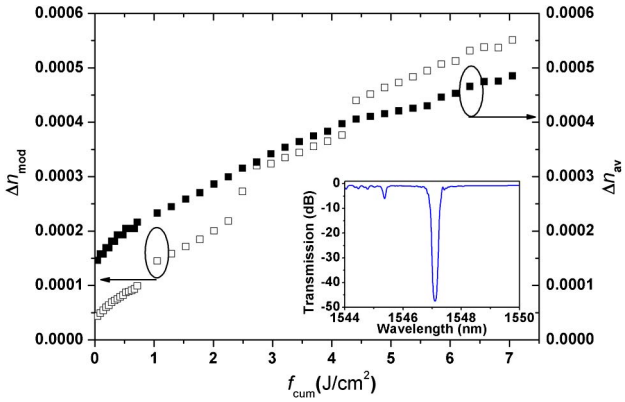

Fig. 1. (Color online) Refractive index changes (squares, Δn_{av}; open squares, Δn_{mod}) as a function of exposure dose for boron-codoped germanosilicate fiber (GF1) irradiated using 193 nm pulsed ArF laser. The inset is the transmission spectrum of one sample fabricated seed grating.

The zero point of the mean refractive index is obtained by measuring the Bragg wavelength after one initial laser pulse. The refractive index modulation change Δn_{mod} can be then calculated from the normalized bandwidth $\Delta\lambda_{\text{bandedge}}$, the Bragg wavelength λ_B, and the effective refractive index n_{eff} [16]:

$$\Delta n_{\text{mod}} = \frac{\Delta\lambda_{\text{bandedge}} \cdot n_{\text{eff}}}{\lambda_B}. \quad (2)$$

The overlap factor is $\eta = 0.8$ with our fiber geometry, and the effective refractive index of the core glass could be derived from the setup as $n_{\text{eff}} = 1.4537$. The inset is the transmission spectrum of one fabricated seed grating with the transmission of ~48 dB. To compare results, twenty seed gratings were fabricated with a typical strength of 48 dB. Figure 2 illustrates the normalized reflection spectra of 10 seed gratings to be regenerated in bulk. The writing conditions were kept identical by applying a constant strain on all gratings. Direct comparison from the normalized reflection gives rise to a small deviation of Bragg wavelength of 0.16 nm. It is noted that the resolution of the optical spectrum analyzer is

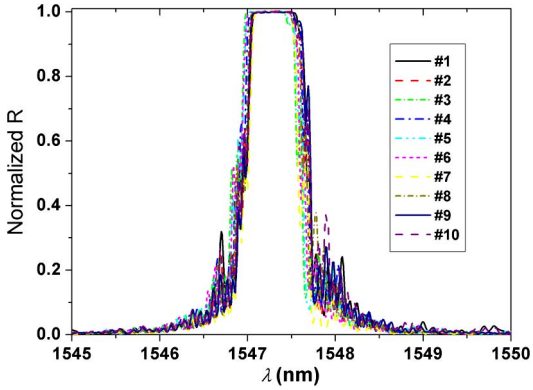

Fig. 2. (Color online) Normalized reflection spectra of 10 seed gratings to be regenerated in bulk (deviation of Bragg wavelength is $\Delta\lambda_B = 0.16$ nm).

~0.06 nm; the observed spread of the Bragg wavelength therefore lies close to within experimental error of the characterization process. Then 10 gratings were tested just after regeneration, while another separate 10 gratings experienced an additional annealing stabilization process.

B. Regeneration Only

Ten seed gratings were mounted onto the stages on either side of the annealing oven (secured ~15 cm away from the hot zone), applying minimal tension to ensure the fiber is straight during the heating of gratings. The isochronal thermal heating schedule for regenerating the GF1 gratings is shown as the red curve in Fig. 3(a) where the temperature of the furnace was raised uniformly from room temperature to $T \sim 850°C$ (the erasing temperature for the seed grating during regeneration) in about 1 h and kept constant at that temperature for 38 min. When the regeneration process is saturated, the furnace was set back to room temperature. Figure 3(b) shows the measured transmission spectra of 10 bulk regenerated gratings. The average Bragg wavelength is $\lambda_B \sim 1546.3$ nm, while the average transmission is $\mathrm{Tr} \sim 1.52$ dB. The variation in Bragg wavelength is only $\Delta\lambda_B \sim 0.41$ nm, while the variation of transmission among 10 regenerated gratings is $\Delta\mathrm{Tr} \sim 0.10$ dB. These are reasonable errors from seed to regeneration. This can in principle be improved, indicating that the grating fabrication and thermal processing system for mass production of regenerated gratings is feasible; i.e., regeneration is a controllable process.

C. Regeneration and Postannealing

Another 10 seed gratings were similarly isochronally annealed for regeneration (same schedule as the first 10 gratings), in this case, however, when the regeneration process had saturated (after $t \sim 120$ min at 850°C), the furnace was heated up to $T = 1100°C$ in $t \sim 20$ min and then kept at this temperature for a further 20 min during the subsequent annealing phase. Figure 4(a) shows the evolution of reflection of a typical grating during regeneration and postannealing process. The normalized reflection decreases from 0.3 to 0.2 due to the high-temperature annealing. The transmission spectra of eight annealed regenerated gratings are shown in Fig. 4(b), where two samples were broken during the experiment. The variation of Bragg wavelength in this case is $\Delta\lambda_B \sim 1.42$ nm, which is notably larger than that of the regenerated gratings without annealing, lying outside experimental variation. However, about 60% of the postannealed regeneration gratings have a wavelength spread of less than 0.35 nm, and it is anticipated that the spread can be reduced if equal tension is applied to all the gratings during the regeneration and postannealing processes, which will be explained further below.

Figure 5 shows the direct comparison of Bragg wavelength deviations, $\Delta\lambda_B$, for three sets of gratings, including seed, regenerated-only, and postannealed ones (note that the seed gratings used for postannealing are not the same ones to those for regeneration only; however, the deviation of Bragg wavelength was also measured to lie within 0.16 nm).

The deviation of regenerated gratings does not follow the pattern of the initial seed gratings, consistent with the seed variation arising from experimental error rather than any systematic effect arising from tension. Nonetheless, the variation in spread among the regenerated gratings suggests that, while there is a fixed tension applied to ensure the fiber is straight during annealing, small variations in this applied tension between gratings exist. With increase in annealing temperature, the spread of the Bragg wavelength progressively worsens from seed to regenerated to postannealing; the postannealed gratings exhibit significant variation. The increasing trend in spread can be explained as arising from the small load the fiber is under, and as the temperature increases the annealing of stress leads to a reduced index, greater confinement, and a longer Bragg wavelength [17]. Fused silica has a stress/strain relief temperature (the temperature at which internal glass stresses are annealed out) of $T_{\mathrm{SR}} \sim 1120°C$ and

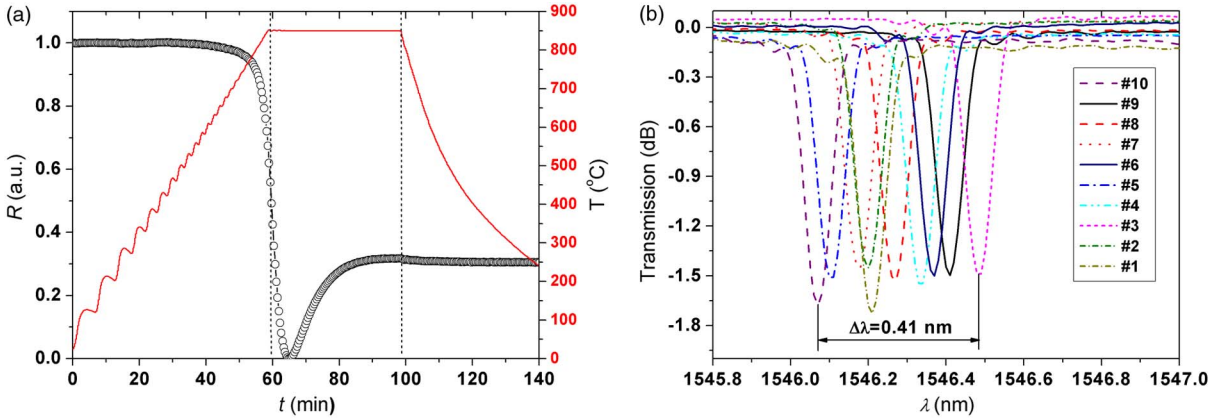

Fig. 3. (Color online) (a) Evolution of reflection of one grating during regeneration process and (b) measured transmission spectra of 10 regenerated gratings.

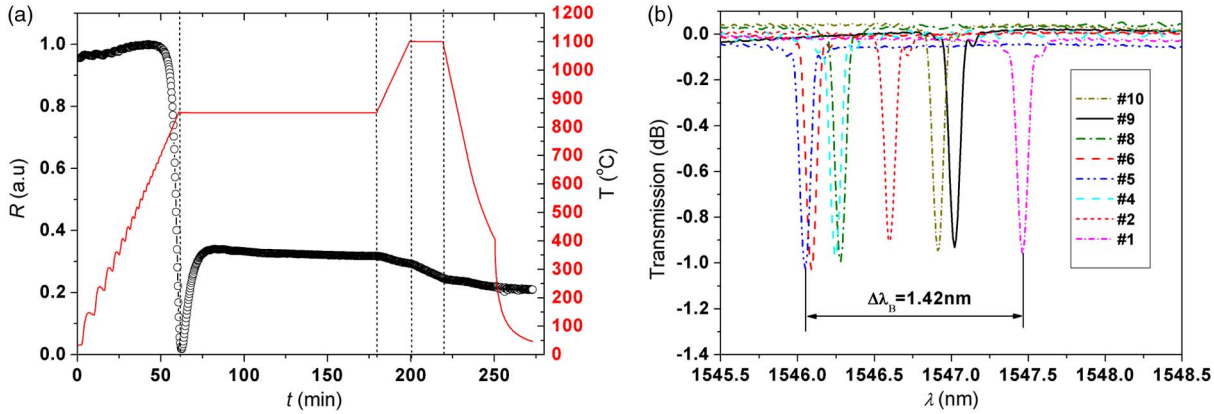

Fig. 4. (Color online) (a) Evolution of reflection of one grating during regeneration and postannealing process and (b) measured transmission spectra of 10 annealed regenerated gratings.

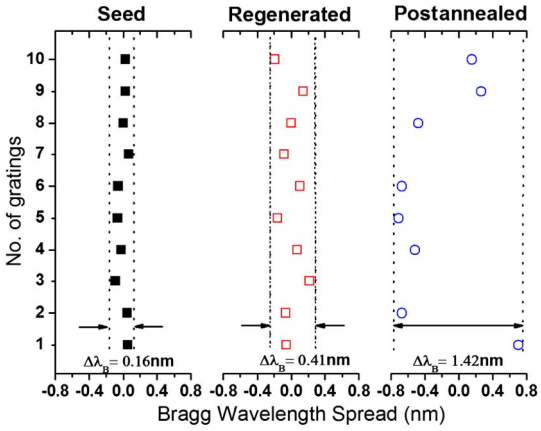

Fig. 5. (Color online) Statistics analysis of Bragg wavelength deviation for three sets of gratings (seed, regenerated, and postannealed).

an annealing point of $T \sim 1215°C$ for Heraeus-like cladding glass [18]. These values will differ given the very rapid quenching of the glass optical fiber during drawing on the fiber draw tower and the fact that the system is a bimaterial system with added core–cladding stresses. Therefore, stresses within the glass itself, frozen in by the rapid quenching of fiber during modified chemical vapor deposition fabrication, are annealed out slowly during our postannealing phase, taking the temperature closer to the strain temperature can accelerate this process. This can reduce the cladding index and core–cladding stresses leading to higher confinement in the core, explaining the apparent rise in index as observed by the grating. By applying a longitudinal load, we are able to relieve stresses more rapidly not only in the cladding but at the core–cladding interface. Lateral compression on the core, which is now soft, may even occur, and this may even lead the core region to elongate and therefore affect the effective pitch of the grating. The contributions of each to the observed profile are to be determined. To reduce the variation of Bragg wavelength of annealed regenerated gratings further, additional precise tension control needs to be integrated into the setup.

3. Conclusions

The reliability and reproducibility of regenerated gratings for mass production has been demonstrated by evaluating 10 bulk regenerated-only, 10 bulk regenerated and, 10 postannealed regenerated gratings. Good reproducibility is obtained although there is some gradual deterioration in wavelength spread from the seed grating to the final structures, with additional postannealing being notably worst off. This is explained by the need for some preexisting tension applied to keep the fiber straight during annealing, which leads to greater change at higher temperatures when the strain temperature of silica is reached or exceeded. Significant room for improving the reproducibility of the applied load itself exists, so we can conclude that the regeneration process is stable and highly reproducible overall. Within reasonable errors, it is amenable to mass production without requiring direct interrogation, thereby offering a route to minimize any additional cost in production over conventional gratings while optimizing high-temperature sensing performance.

This project acknowledges Australian Research Council (ARC) funding. L. Shao acknowledges the award of an Australia Award Endeavour Research Fellowship, the Hong Kong Polytechnic University project G-YX5C, and the National Natural Science Foundation of China under grant 61007050. T. Wang acknowledges the China Scholarship Council visiting scholar award.

References

1. D. Inaudi and B. Glisic, "Fiber optic sensing for innovative oil and gas production and transport systems," in *Optical Fiber Sensors*, OSA Technical Digest (CD) (Optical Society of America, 2006), paper FB3.
2. S. J. Mihailov, "Fiber Bragg grating sensors for harsh environments," Sensors **12**, 1898–1918 (2012).
3. M. L. Aslund, N. Jovanovic, S. D. Jackson, J. Canning, G. D. Marshall, A. Fuerbach, and M. J. Withford, "Photo-annealing of femtosecond laser written Bragg gratings," in *Joint Conference of the Opto-Electronics and Communications Conference, 2008 and the 2008 Australian Conference on Optical Fibre Technology, OECC/ACOFT 2008*, 7–10 July 2008 (IEEE, 2008), pp. 1–2.

4. Y. Shen, J. He, Y. Qiu, W. Zhao, S. Chen, T. Sun, and K. T. Grattan, "Thermal decay characteristics of strong fiber Bragg gratings showing high-temperature sustainability," J. Opt. Soc. Am. B **24**, 430–438 (2007).
5. M. L. Åslund, J. Canning, M. Stevenson, and K. Cook, "Thermal stabilization of type I fiber Bragg gratings for operation up to 600°C," Opt. Lett. **35**, 586–588 (2010).
6. Y. Li, M. Yang, D. N. Wang, J. Lu, T. Sun, and K. T. V. Grattan, "Fiber Bragg gratings with enhanced thermal stability by residual stress relaxation," Opt. Express **17**, 19785–19790 (2009).
7. M. Åslund and J. Canning, "Annealing properties of gratings written into UV-presensitized hydrogen-outdiffused optical fiber," Opt. Lett. **25**, 692–694 (2000).
8. N. Groothoff and J. Canning, "Enhanced type IIA gratings for high-temperature operation," Opt. Lett. **29**, 2360–2362 (2004).
9. D. Grobnic, C. W. Smelser, S. J. Mihailov, and R. B. Walker, "Long-term thermal stability tests at 1000°C of silica fibre Bragg gratings made with ultrafast laser radiation," Meas. Sci. Technol. **17**, 1009–1013 (2006).
10. S. Bandyopadhyay, J. Canning, M. Stevenson, and K. Cook, "Ultrahigh-temperature regenerated gratings in boron-codoped germanosilicate optical fiber using 193 nm," Opt. Lett. **33**, 1917–1919 (2008).
11. J. Canning, M. Stevenson, S. Bandyopadhyay, and K. Cook, "Extreme silica optical fibre gratings," Sensors **8**, 6448–6452 (2008).
12. E. Lindner, C. Chojetzki, J. Canning, S. Brückner, M. Becker, M. Rothhardt, and H. Bartelt, "Thermal regenerated type IIa fiber Bragg gratings for ultra-high temperature operation," Opt. Commun. **284**, 183–185 (2011).
13. J. Canning, "Regenerated gratings for optical sensing in harsh environments," in *Bragg Gratings, Photosensitivity, and Poling in Glass Waveguides*, OSA Technical Digest (online) (Optical Society of America, 2012), paper Btu3E.3, invited.
14. J. Canning, "Fibre gratings and devices for sensors and lasers," Laser Photon. Rev. **2**, 275–289 (2008), invited review.
15. S. Bandyopadhyay, J. Canning, P. Biswas, M. Stevenson, and K. Dasgupta, "A study of regenerated gratings produced in germanosilicate fibers by high temperature annealing," Opt. Express **19**, 1198–1206 (2011).
16. T. Erdogan, "Fiber grating spectra," J. Lightwave Technol. **15**, 1277–1294 (1997).
17. L. Y. Shao, T. Wang, J. Canning, and K. Cook, "Regenerating gratings under strain," to be presented at the 37th Australian Conference on Optical Fibre Technology, Sydney, Australia, 9–13 December 2012).
18. http://www.newrise-llc.com/fused-silica.html.